# Helium Bubble Visualization of the Tip Vortex

A. Vinckier
R. Stangl
L. Zerle
S. Wagner
Institut für Aerodynamik und Gasdynamik
Universität Stuttgart

Abstract

The helium bubble technique is a new method for the visualization of the tip vortex geometry. It is based on the injection of soap bubbles containing helium at the rotor tip. The helium serves as a bouyancy medium. The bubbles remain lighter than air and are therefore trapped inside the vortex core. Unlike smoke, the helium bubbles do not diffuse and are therefore still able to indicate the vortex geometry far downstream. Results are presented for a helicopter in hover and the vortex-wing-interaction of a hovering and tilting rotor.

## 1. Introduction

Vortex geometry of a rotor wake is one of the most interesting features in helicopter aerodynamics and performance. The knowledge about the downwash structure is essential for two aspects: Blade-vortex-interaction (BVI) which is responsible for noise and high frequency vibrations, and rotor-fuselage-interaction (RFI), with effects like vortex impact to canopy, tail rotor and fin.
Several activities in rotor wake visualization [1] were undertaken to generate data bases for computer programs which handle prescribed wake models. Actual CFD developments like EULER codes with wake capturing capability [2, 3] and free wake vortex lattice methods [4, 5] aim to handle interaction aerodynamics and special flight conditions like descent. Code validations will require details of rotor wake structure especially in this conditions, too. In addition, the visualized wake vortices are important for modern helicopter concepts like higher harmonic blade control, individual blade control and future methods in rotor torque compensation.

The helium bubble visualization technique was first developed at the University of Gent in cooperation with Westland Helicopter as part of a Master thesis [6]. It was then clear that this is an effective technique. The second prototype was developed at the University of Stuttgart and included improved control systems and a novel bubble generator.

## 2. Dynamical structure of a vortex

The dynamical structure of a trailing vortex consists of two regions. The first is called the 'region of persistence' and the second is called the 'region of vortex decay'.
The region of persistence is characterized by the axial acceleration of the fluid in the vortex core from zero velocity to the free stream velocity. This axial acceleration causes a radial inflow which is larger than the radial diffusion velocity. This makes the vortex stable and persistent. Once the axial acceleration is terminated the vortex starts to decay. The lack of radial inflow causes the vortex to diffuse. For a rotor tip the length of the region of persistence vortex is on the average 1 to a maximum of 2 two rotor rotations long.

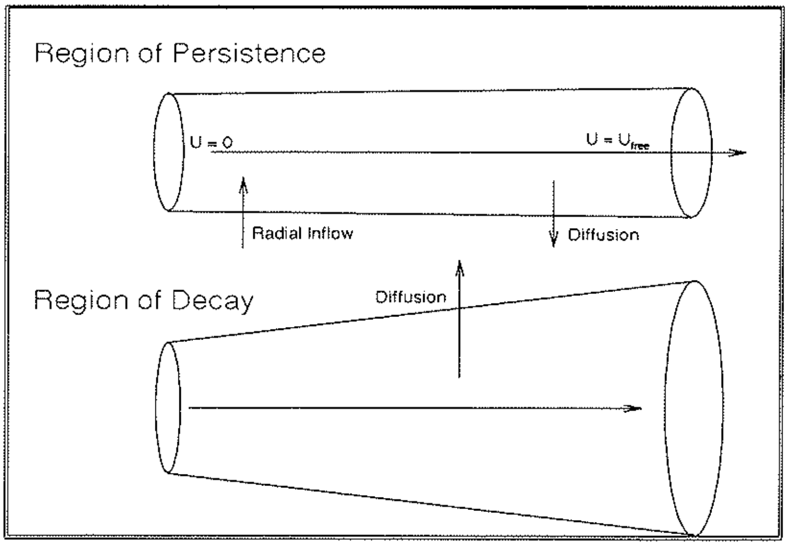

Figure 1 Vortex Structure

Particles, such as smoke or moisture, which are in the vicinity of a vortex are able to remain in the vortex core for a short time. This phenomenon is described by Roberts [7]. Two forces act on a particle. The circular motion around a vortex causes a centrifugal force. This force is counteracted by the drag acting on the particle due to the radial inflow. The particle will find a radius along the vortex where those two forces are in balance. The inward radial velocity is small near the vortex centre which moves the particle to a larger radius. Thereby, the typical tube like structure is obtained for smoke or moisture around a vortex. The particles diffuses rapidly once the vortex starts to decay.
It is therefore important for new visualization techniques to take the structure of the vortex into account and to avoid the influence of vortex decay (the lack of inward radial flow).

## 3. Visualization methods

### 3.1 Water tunnel visualization

The visualization is realized either by cavitation or by injection of air. Tip vortices of ship propellers are frequently visible if cavitation pressure in the vortex core is obtained.
Lehman [8] has visualized the rotor tip vortices with the injection of air at the rotor tip, thereby avoiding cavitation corrosion on the models. Air or steam in the vortex core stay far beyond the start of vortex decay. The pressure gradient in a vortex forces the lower density air or steam to remain confined in the vortex core, and is therefore free of the diffusion influences. The problems associated with water tunnel visualization are: water tunnels are rare, the models undergo very high forces and cavitation occurs.

### 3.2 Visualization by condensation

A strong pressure drop in the vortex core together with the right amount of moisture causes condensation in the vortex core. This condense remains visible as long as the vortex is in the region of persistence, thereafter the condense centrifuges out. Under normal condition the vortex core is visible for 1 to 2 rotor rotations, for extremely heavy loaded helicopters the vortex can be seen for up to three rotation. This visualization has not yet been used in wind tunnels, but the authors believes that it can give good results if the climate in the wind tunnel is controllable. A great advantage of this method is that no modification of the rotor model are needed.

### 3.3 Smoke visualization

Smoke visualization is the evident technique for vortex visualization. But this technique is vulnerable to the vortex decay and can therefore hardly be used beyond 2 rotor rotations. Its implementation requires tubing in or around the rotor shaft and in the rotor blades or a smoke feeding probe nearby the rotor disk. Smoke generators are readily available.

A new smoke visualization method has been developed by Müller [9]. This method is based on very small burning titanium particles which are shot through the airflow of interest. Those burning particle produces a fine smoke track. The displacement of the smoke track gives a good idea of the flow field.

### 3.4 Optical methods

The significant pressure drop in the vortex reduces the density. This density change allows the application of Schlieren (J. Tangler [10]) or schadowgraphy (Parthasarathy [11], Leishman [12]). Those methods give good results but its observation is severely limited by the dimensions of the optical apparatus.

Laser Doppler Anemometry (LDA) and Particle Image Velocimetry (PIV) give excellent flow field data, but requires particle seeding and an intensive computer post processing to locate vortex positions in the flow field.

### 3.5 Helium bubble visualization

The use of soap bubbles filled with helium allows two things. First, they are very persistent (they remain visible for several minutes). Second, the lighter than air bubbles are pushed to the vortex centre through the pressure gradient. The helium bubbles remain visible far beyond the start of vortex decay and due to the favourable pressure gradient remain well inside the vortex core. The rotation of the bubbles around the vortex axis and the axial airflow acceleration in the vortex core is clearly visible. The displacement vector, or velocity vector can be determined by trakking the individual bubbles. Stereo photography will allow to obtain 3-D data of the vortex position. A further advantage is that only one tip vortex is visualized which makes the pictures, hence the data acquisition, less complex.

The disadvantage of this method is the low visibility of the helium bubbles. Extreme care must be taken with light and background illumination. A practical discomfort is the pollution of the hardware by the soap liquid, which causes corrosion of the rotor model and makes the wind tunnel extremely slippery. The special equipment for helium and soap and its introduction in the rotor construction makes the system more complex.

## 4. Description of the Rotor Testbed / Technical Capability

### 4.1 General Information

The method of vortex visualization by helium bubbles is applied to a 2 bladed, 2.10 m diameter fully articulated rotor as given in figure 2.

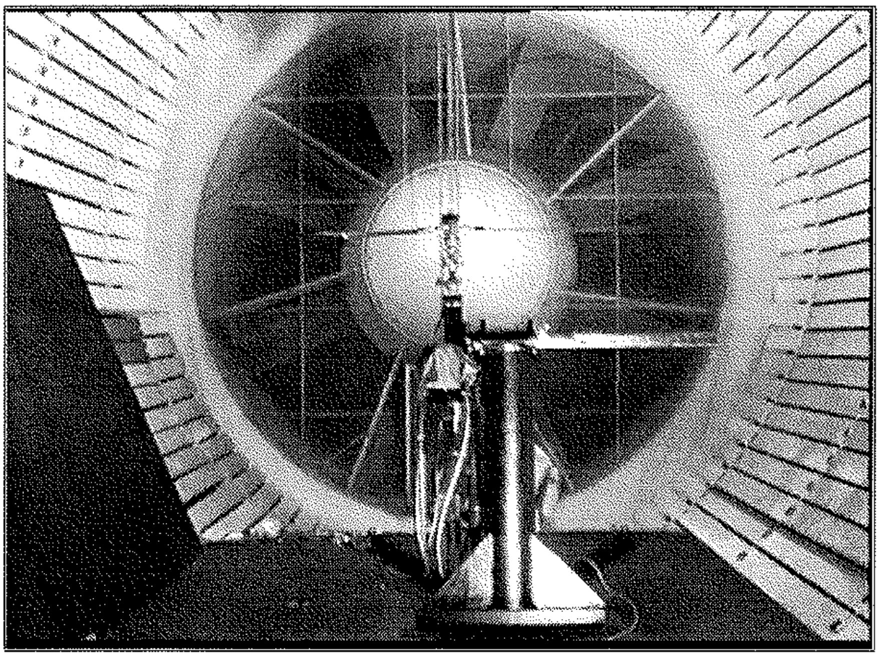

Figure 2 Front View of the Testbed

The whole apparatus is placed in the institutes wind tunnel which has a diameter of 6.3 m and gives the possibility to investigate helicopter forward flight and tilt rotor transitions. This wind tunnel is designed to simulate gust wind on models (e.g. windmills) and has therefore an extreme large turbulence grade. The rotor system and its hydraulic powered driving unit are fixed on a girder, which can be tilted around the top of a strong steel pillar. The tilt ranges from horizontal rotor position to propeller forward flight position. The whole configuration with its tilting limits is drawn in figure 3 and 5. Rearward tilting allows to investigate helicopter descent flight conditions.

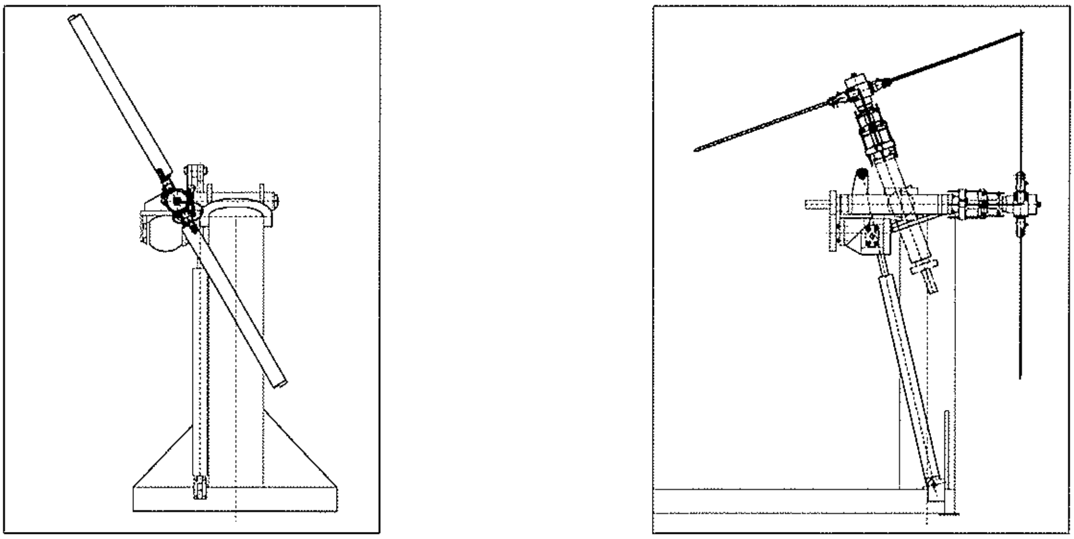

Figure 3 CAD-Construction of the Rotor

Rotor blade control is done by a roller bearing swash plate (figure 4). In the actual development stadium collective and cyclic pitch must be adjusted by hand at the non rotating swash plate face. This is sufficient for the verification of the visualization method and for the improvement of critical testbed components. Future upgrading will consist in actuator controlled operations with the option of rotor trim in forward flight. The rotor blades are of composite material with maximum stiffness.

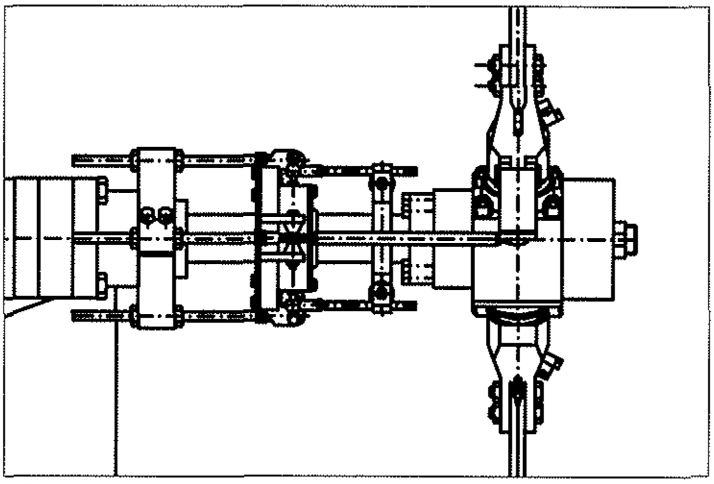

Figure 4 CAD-Construction of the Rotor - Close-up

Bodies, such as fuselages and wings, (figure 5) can be mounted in the vicinity of the rotor downwash area in order to investigate complex interactional vortex behaviour.

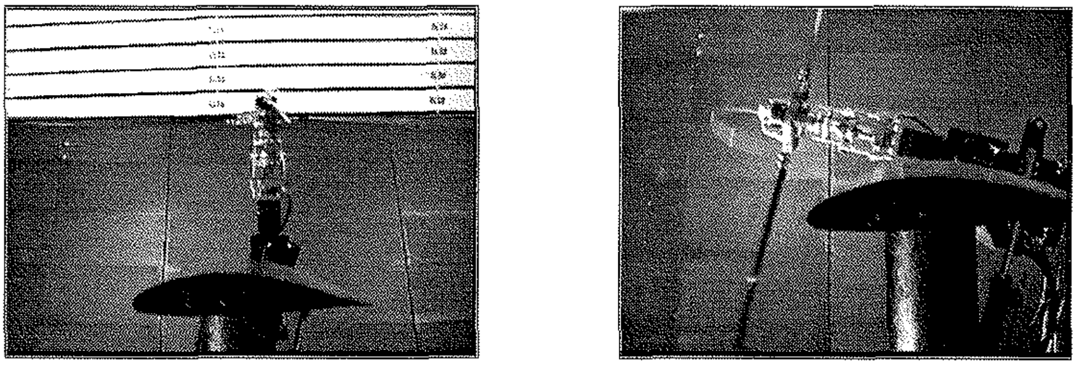

Figure 5 Side View of Rotor with Wing - Vertical and Horizontal Rotor Axis

| | | |
|---|---|---|
| Number of blades | | 2<br>untwisted, one equipped for helium bubble feed |
| Airfoil section | | NACA 0015, constant along span |
| Rotor radius | R | 1.05 meter |
| Hinge offset | r/R | 0.028<br>without pitch-flap coupling |
| Root cut-out | r/R | 0.20 |
| Airfoil chord | | 0.07 meter |
| Range of rotor tilting angle | | -90° to +20° (0°= Hover) |
| Rotor plane above floor | | 2.1 R |
| Blade stiffness | | Maximum |
| Blade weight | | 0.450 Kg |
| Wind tunnel speed | | 20 m/s max. |
| Wind tunnel diameter | | 6.3 meter |

The rotor and testbed construction was done in the frame of a Diploma Thesis [13] at the Institut für Aerodynamik und Gasdynamik, special attention was given to the incorporation of the helium-soap equipment and to the adaptability for future investigations.

## 4.2 Installations for Helium Bubble Production

To achieve good results, helium and bubble liquid must be mixed near by the location of bubble release to the free air. It is necessary to place the bubble generator at the tip region within one rotor blade and to feed the mixing unit by two separate tubes. The Helium comes from a pressure bottle, passes a flow control valve and flows through the hollow rotor shaft to one of the tubes in the rotor blade. An axial sealed element around the shaft is used for helium transfer into the rotating system. Bubble liquid support is given by a small tank mounted at the top of the rotor hub. A second tube in the blade feeds the liquid under centrifugal force through a fluid regulation valve to the bubble generator. Due to high radial pressure gradients along the blade span it is necessary to position this valve at the outer position. The quality of the bubble string along the vortex core is very sensitive to valve control input and rotational speed. Liquid mixture, fluid valve and helium fluid mixing unit are still to be improved.

## 5 Experiments and Results

Result acquisition was done primarily by video camcorders in different view positions with 1/1000 of a second shutter time. To obtain high contrast pictures of the bubble lines the test-bed illumination and background darking is very important and critical. In addition, picture post processing and preparation i.e. contrast manipulation for printed images was performed on a Silicon Graphics Indy workstation. Another influence to picture quality are the helium/fluid mixing and ejection conditions. There is a considerable influence on picture quality when additional non vortex core located bubbles (fluid overcharged, heavier than air bubbles) are present in the flow field or not. In a future step pictures from different view points will be taken simultanously to enable three dimensional vortex position evaluation by analysing the stereoscope pictures with a computer program. These results will for example be used for CFD-code validation.

### 5.1 Isolated Rotor in Hover

A first test was performed with a rotor speed of 250 rpm (= 28 m/s tip speed) and a collective pitch of 10° and is documented in figure 6. During good conditions up to 5 full rotations of stable helical vortex track were observable, until the downwash is spreaded by the ground. Expected helix line contraction occurred. Bubble self rotation was visible and underlines that the bubble track is a real representation of the vortex core line.

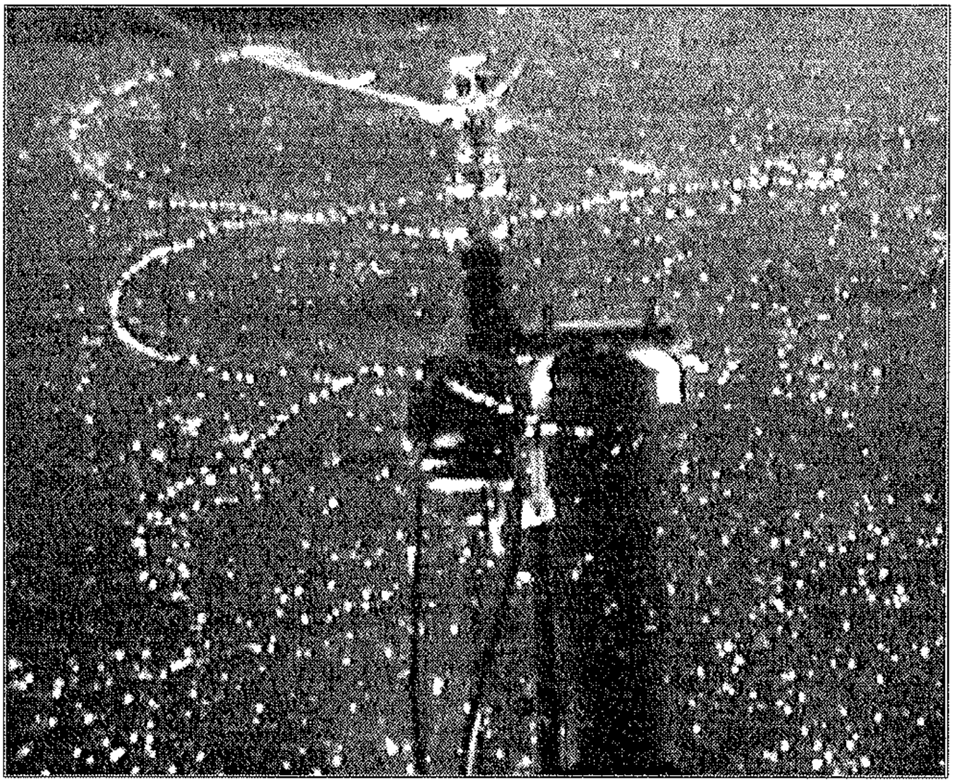

Figure 6 Tip Vortex Structure - Front View

## 5.2 Interaction Tests in Hover

Tip vortex behaviour at surface approach was investigated by placing a wing section in the rotor downwash area. The profile was located 0.7 meters below the rotor as shown in figure 7 and 8.

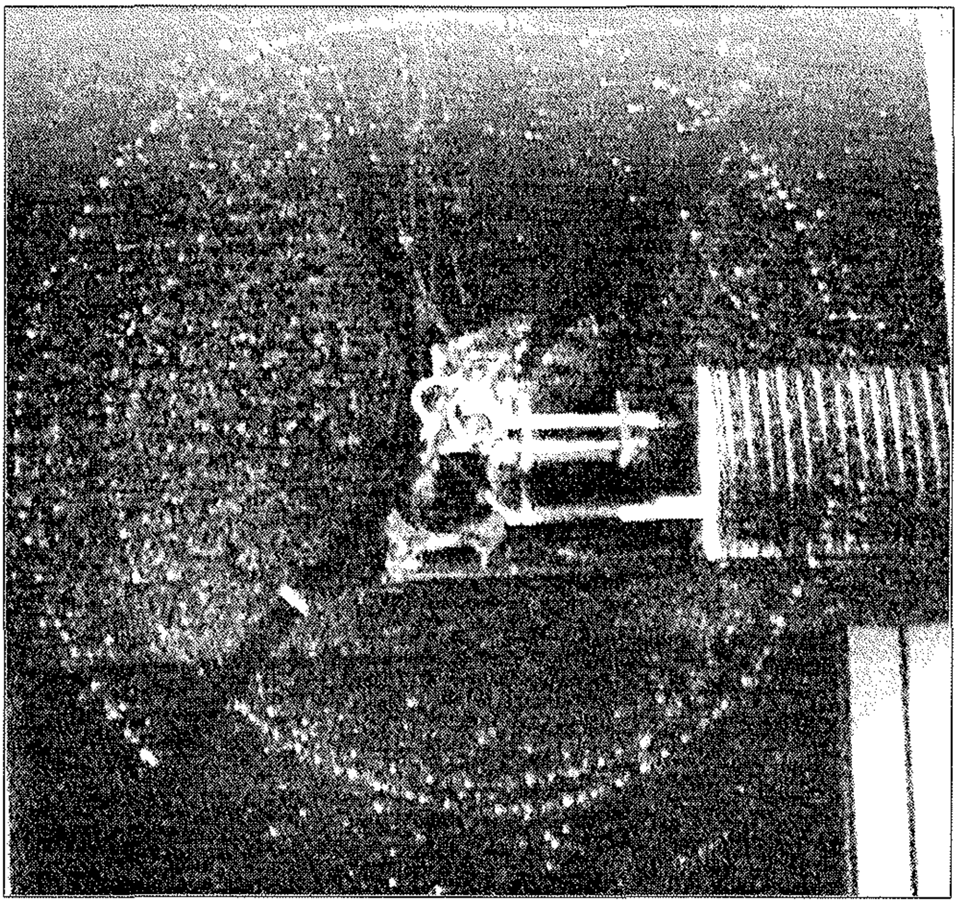

Figure 7 Vortex-Wing-Interaction - Top View

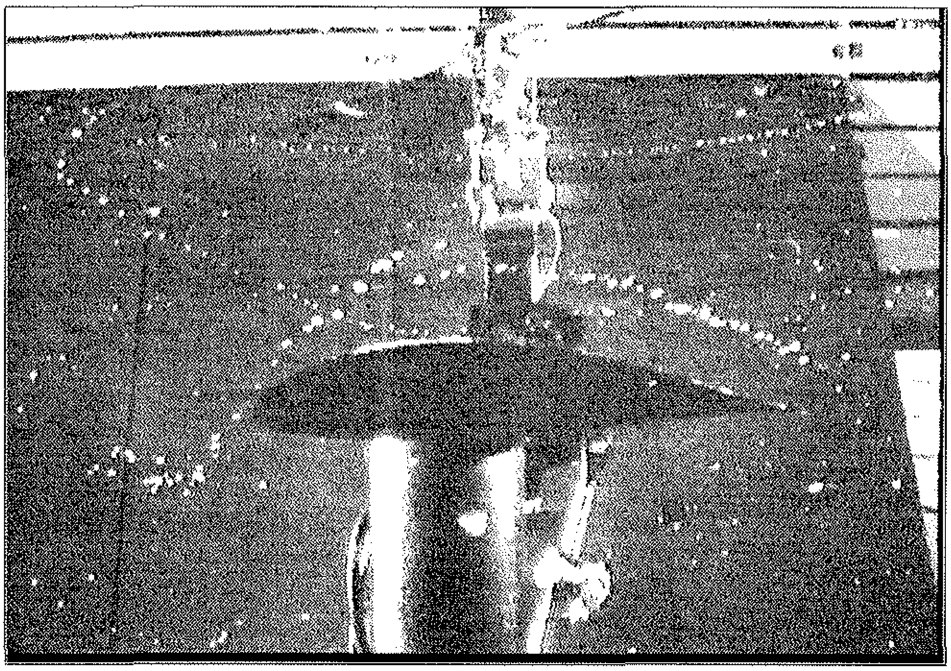

Figure 8 Vortex-Wing-Interaction - Side View

Due to the excellent bubble persistence two effects could be observed:

a) If the tip vortex approaches to the upper wing surface, it loops out in a U-shape towards the outer direction (figure 7). This is a well known effect of vortex reaction. The vortex line acceleration and speed of deformation in the vicinity of the wing is surprisingly high, which is documented on a video.

b) The vortex wing distance during its outer movement above the wing is visible in figure 8, and seems to remain at a distinct value during the pass by.

In figure 9 a sequence is presented showing the vortex wing interaction from a rear view. Picture one defines the viewpoint behind the wing together with the vertical rotor axis at the right side. The following 8 images are taken from a video and are computer processed. They are colour inverted and the contrast is enhanced. The visibility of the vortex, wing and rotor blades is thereby increased. The sequence shows exactly a single rotor rotation. One can see a tip vortex descending down to the wing and locally accelerating in horizontal direction along the wing. At the end of the wing the vortex intends to move upwards and decays as observed in the side view camera position.

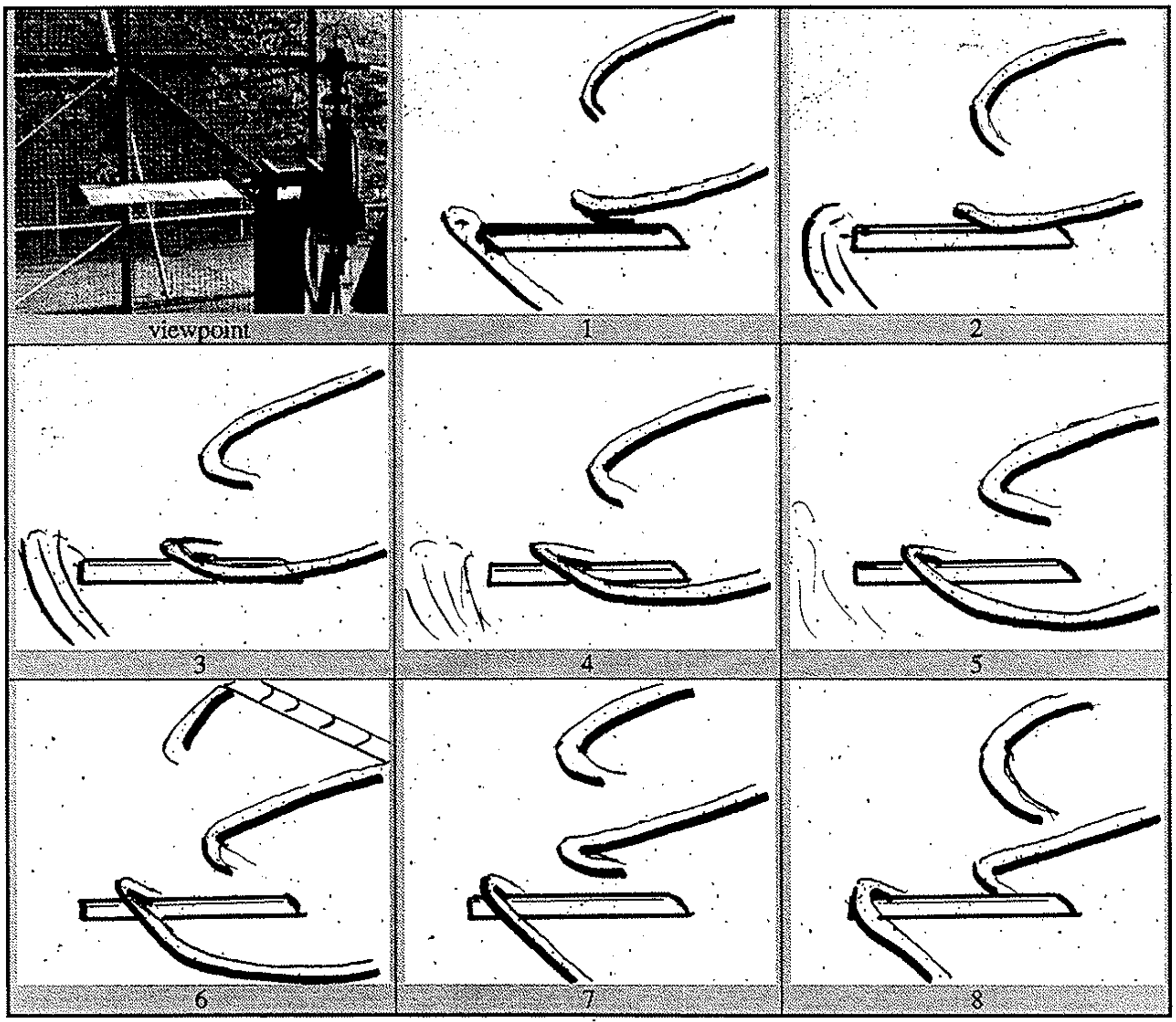


Figure 9 Vortex-Wing-Interaction - Rear View

### 5.3 Rotor Tilt Tests

Figure 10 presents the visualization result at the transition position 75° near propeller mode. The vortex cut at wings leading edge results in a kind of vortex contraction at about half a chord length above the wing.

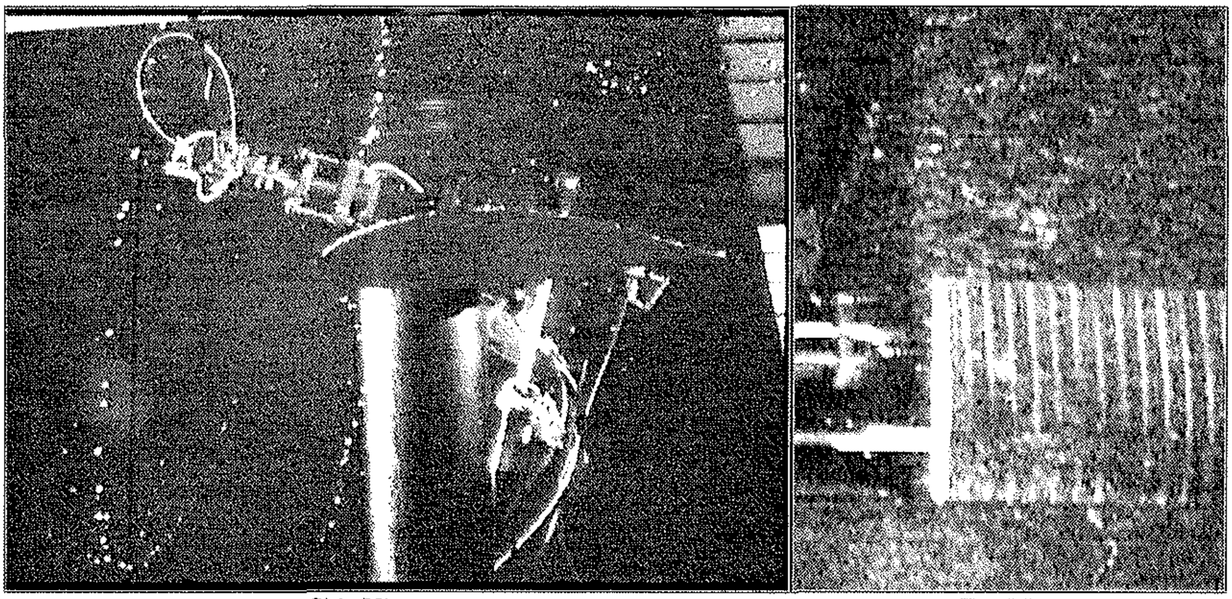

Side View Top View

Figure 10 Vortex Wing Interaction - 75° Tilt Angle

In Figure 11 presents the side view for a transition angle of 55°, where the vortex impinges on the leading edge.

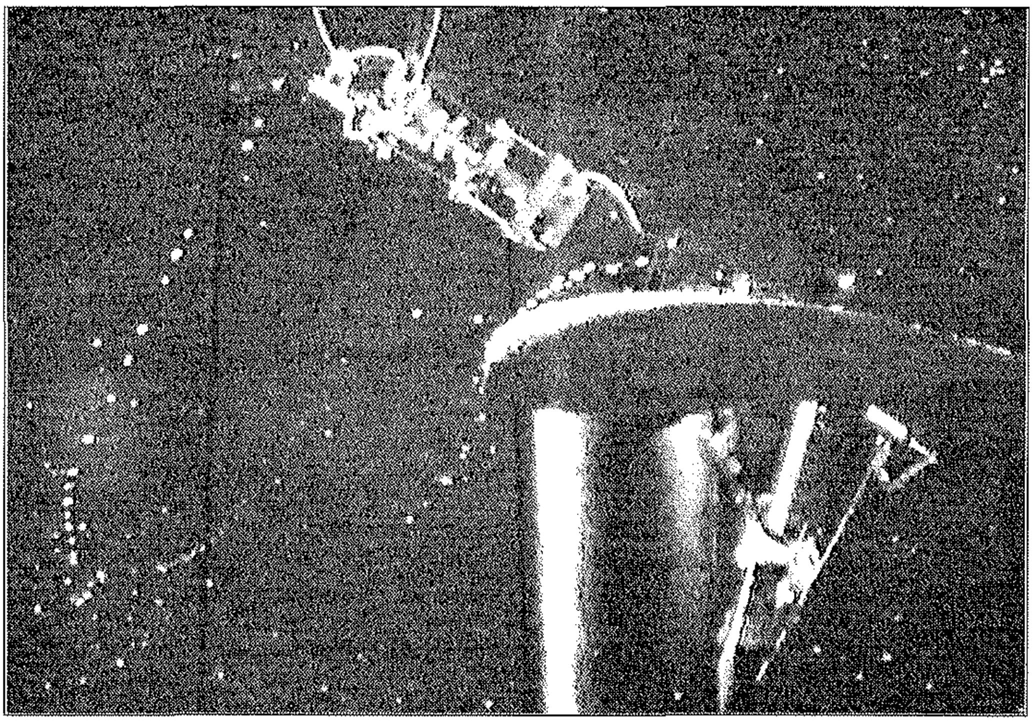

Figure 11 Vortex Wing Interaction - 55° Tilt Angle

## 7 Conclusions

The results, which have been so far obtained, demonstrate the validity of the helium bubble visualization technique. The main characteristic is the long tracking of vortices, which allows instant 3-D observations of complex vortex geometries, and the tracking of individual bubbles for velocity acquisition. This permits the investigation of rotor-fuselage-interaction, of blade-vortex-interaction, vortex-wing-interaction. This technique can certainly be applied to other complex vortex flows.

## References


[1] A. Landgrebe. *The Wake Geometry of a Hovering Helicopter Rotor and its Influence on Rotor Performance.* Paper Presented at the 28th Annual National Forum of the American Helicopter Society, May 1972.

[2] J. Hertel, E. Krämer und S. Wagner. *Complete Euler Solution for a Rotor in Hover and a Propeller in Forward Flight.* Paper Presented at the 16th Eurpean Rotorcraft Forum, Glasgow, Scottland, 18.-21. September 1990, Proceedings, Paper No. 2.6.

[3] R. Stangl und S. Wagner. *Euler Calculation of the Flow Field Around a Helicopter Rotor in Forward Flight.* Paper Presented at the 20th Eurpean Rotorcraft Forum, Amsterdam, The Netherlands, 4.-7. October 1994, Proceedings, Paper No. 38.

[4] L. Zerle und S. Wagner. *Influence of Inboard Shedded Rotor Blade Wake to the Rotor Flow Field.* Paper Presented at the 19th Eurpean Rotorcraft Forum, Como, Italy. September 1993, Proceedings, Paper No. C13.

[5] A. Röttgermann, R. Behr, Ch. Schöttl und S. Wagner. *Calculation of Blade-Vortex Interaction of Rotary Wings in Incompressible Flow by an Unsteady Vortex Lattice Method Including Free Wake Analysis.* In Hackbusch W., editor, Notes on Numerical Fluid Mechanics, pages 153-166, Braunschweig, 1991, Vieweg Verlag.

[6] A. Vinckier. *Visualisatie van de Tipwervel van een Helikopterrotor.* Diploma Thesis Rijksuniversiteit Gent Belgium 1986.

[7] L. Roberts. *On the Structure of the Turbulent Vortex.* AGARD-CP-342 paper 3, April 1983.

[8] A. Lehmann. *Model Studies of Helicopter Rotor Flow Patterns.* USAAVLABS Technical Report 68-17.

[9] R. Müller. *Measurement of Helicopter Rotor Tip Vortices using the Flow Visualization Gun - Technique.* Paper Presented at the 18th Eurpean Rotorcraft Forum, Avignon, France, 15.-18. September 1992, Proceedings, Paper No. 82.

[10] J. Tangler. *Schlieren and Noise Studies of Rotors in Forward Flight.* Preprint No. 1004, 33rd Annual National Forum of the American Helicopter Society, May 1977..

[11] S. Parthasarathy. *Wide-field Shadowgraph Flow Visualization of Tip Vortices Generated by a Helicopter Rotor.* AIAA-85-1557, July 1985.

[12] J. Leishman, G. Crouse and N. Bi. *Theoretical and Experimental Study of Unsteady Rotor/Body Aerodynamic Interactions.* Paper Presented at the 46th Annual National Forum of the American Helicopter Society,, Washington, DC, May. 1990.

[13] A. Wild. *Konstruktion einer Hubschrauberversuchsanlage zur Visualisierung von Blattspitzenwirbeln.* Diploma Thesis, Universität Stuttgart, October 1994.